COBEM 2021 26th International Congress of Mechanical Engineering
November 22-26, 2021, Virtual Congress, Brazil
ABCM Associação Brasileira de Engenharia e Ciências Mecânicas

# COB-2021-1038
# DISPERSION ANALYSIS OF STRONGLY NONLINEAR MAGNETOELASTIC PERIODIC STRUCTURES USING HBM-AFT METHOD

**Matheus Basílio Rodrigues Fernandes**
**Thiago de Paula Sales**
**Domingos Alves Rade**
Department of Mechanical Engineering, Aeronautics Institute of Technology, Pç. Mal. Eduardo Gomes, 50, São José dos Campos, SP 12228-900, Brazil
engmatheusb@gmail.com, tpsales@ita.br, rade@ita.br

***Abstract.*** *This paper addresses wave propagation in one-dimensional magnetoelastic periodic chains, which are known to exhibit strongly nonlinear dynamical behavior. A modification of the standard harmonic balance method adapted to wave propagation problems is proposed to deal with complicated nonlinear forces in a computationally efficient way. In this approach, known in the literature as the Alternating Frequency-Time scheme, the inverse and direct discrete Fourier transforms are used to effectively evaluate the residual of the harmonic balance equation. Different arrangements of permanent magnets are explored to produce unit cells with various dynamic behaviors, with both softening and hardening interaction forces. The study reveals amplitude-dependent dispersion relations, which makes it possible to design structures with tunable filtering properties.*

***Keywords:*** *nonlinear periodic structures, amplitude-dependent dispersion, wave propagation, harmonic balance method, alternating frequency-time scheme*

## 1. INTRODUCTION

Whether in the form of phononic crystals or metamaterials, periodic structures are systems that have the ability to manipulate the propagation of elastic and acoustic waves in material media. They can also exhibit remarkable dynamical properties, often not found in naturally occurring materials, such as negative effective properties (Huang *et al.*, 2009; Wang, 2014). The most prominent feature of these lattice structures is the existence of frequency bands where mechanical waves cannot propagate freely, even in the absence of damping. These frequency bands, called band gaps, pave the way for the use of these structures as vibration and noise isolators, waveguides, acoustic cloaking, seismic isolation, to name but a few (Hussein *et al.*, 2014).

There are two main physical mechanisms responsible for the formation of band gaps. One is the Bragg interference, in which forward and backward propagating Bloch waves interfere destructively at wavelengths comparable to the characteristic size of the lattice (Brillouin, 2003; Laude, 2020). The other mechanism is related to the existence of a resonating system within the unit cell (Liu, 2000). In this case, the frequency range of the band gap is dictated by the resonance frequency of the oscillator, rather than by the periodicity of the lattice, opening up the possibility of creating band gaps at lower frequencies, without the limit imposed by the length of the unit cell.

Although the study of metamaterials and phononic crystals has been attracting the attention of scientists and engineers due to their potential technological applications, the vast majority of investigations focus on linear analysis. However, taking the nonlinear effects into account allows for a more accurate description of the underlying dynamics, especially when large deformations and strains need to be taken into account. Furthermore, the nonlinear world presents some interesting phenomena with no counterpart in the linear regime, such as solitary waves, internal resonances, chaos, harmonic generation, amplitude-dependent dispersion, etc. (Theocharis *et al.*, 2013; Manktelow *et al.*, 2017). One calls attention to the latter, since the dispersion relation is a key part in the investigation of wave propagation in periodic structures. As it establishes a link between wave frequency and wavenumber, the dispersion diagram allows one to determine the frequency ranges associated with band gaps.

In this sense, recent studies have developed techniques for correcting the dispersion diagram given the existence of nonlinear interactions. Narisetti *et al.* (2010) and Narisetti *et al.* (2011) developed a perturbation approach for predicting the dispersion properties of 1D and 2D weakly nonlinear periodic structures. Analyzing systems with cubic nonlinearities, they obtained analytical expressions for the dispersion diagram and showed its dependence on the amplitude of motion. Manktelow *et al.* (2013) extended this methodology to deal with multi-degree-of-freedom systems discretized using the

finite element method. The works of Cabaret *et al.* (2012) and Manktelow *et al.* (2014) report experimental evidence of the amplitude dependence of the dispersion properties of a wire-mass system and a diatomic granular chain, respectively, subjected to weak nonlinear effects. Although these works have dealt with weakly nonlinear systems, structures subjected to the action of strong nonlinear phenomena have also been investigated. Narisetti *et al.* (2012) studied the propagation of waves in strongly nonlinear 1D and 2D periodic media using the harmonic balance method (HBM). Their analysis showed that the width and center frequency of the band gaps, as well as the group velocity, are amplitude-dependent. This approach has been validated for chains of spheres in contact, modeled using Hertz's theory, by direct time-domain simulations. Wei *et al.* (2020) also studied lattice structures comprising contact phenomena described by Hertz's theory. They applied the incremental harmonic balance method (IHBM) to determine the dispersion properties and studied the diode phenomenon in the 1D diatomic lattices which were investigated. In another work, Wang *et al.* (2020) converted the equation of motion of a 1D monoatomic periodic system to a corresponding delay differential equation, with time delays and advances, which was analyzed using the IHBM technique. More recently, Song and Zhu (2021) extended this methodology to diatomic mass-in-mass chains with cubic nonlinearities.

Since the nonlinear dispersion properties provide a powerful characterization of wave propagation over large amplitudes, this work proposes a new methodology for the calculation of the dispersion relation of strongly nonlinear periodic structures. The method is based on an extension of the traditional HBM from nonlinear vibration to problems involving wave propagation. To deal with complicated nonlinear forces in a computationally efficient way, we make use of the Alternating Frequency-Time (AFT) scheme, which applies the discrete Fourier transform (DFT) (in its inverse and direct forms) to approximate the Fourier coefficients of the nonlinear terms. Issues related to accuracy, convergence and computational efficiency of the proposed methodology are also addressed. The method is illustrated through the study of monoatomic periodic structures on an elastic foundation, whose unit cells are composed of attracting and/or repelling permanent magnets (PMs). This type of system is chosen to illustrate the methodology's ability to deal with nonlinearities described by not so simple expressions in a straightforward way, unlike previous studies, which dealt with nonlinear forces given by simpler analytic expressions.

The remainder of this paper is organized as follows. First, the model adopted for assessing the interaction forces between PMs is presented (Sect. 2.1). Then, the HBM applied to wave propagation problems is presented (Sect. 2.2), followed by a discussion of the AFT scheme (Sect. 2.3) and the choices for the phase condition and amplitude normalization (Sect. 2.4). Next, one presents a methodology to evaluate the dispersion relation for nonlinear periodic structures (Sect. 2.5), and its application to monoatomic repelling (Sect. 3.1) and attracting (Sect. 3.2) magnetoelastic chains. Finally, concluding remarks are presented.

## 2. MATHEMATICAL MODELING

### 2.1. Model for the interaction force between permanent magnets

The interaction forces between PMs are inherently nonlinear. Many models which characterize their behavior can be found in works dealing with applications of PMs. Simplified models which assume the interaction forces decay with distance following an inverse power law are common in the literature. Although very simple and relatively easy to work with, these models lack a theoretical framework based on the laws of physics and, therefore, raise doubts about the limits of their applicability.

On the other hand, there exist models which are completely based on first principles for the magnetic field generated by PMs and the associated interaction forces. In particular, for PMs with simple geometry (like cuboidal or cylindrical), analytical expressions have been derived. Within this context, the magnetic surface charge model (Janssen, 2011) is adopted here. From a magnetostatic analysis and by using a scalar potential derived from Maxwell's equations, this model replaces the volumetric distribution of the magnetic field of a PM with fictitious magnetic surface charge distributions on the two surfaces normal to its magnetization. These surfaces are highlighted in gray in Fig. 1a. These magnetic charge surfaces, although a mathematical abstraction with no clear physical interpretation, can be shown to produce the same magnetic field as the original PM. The main hypotheses assumed by the model are that the magnetization is homogeneous and the relative permeability is unitary within the PM. The reader is refereed to Janssen (2011) for more details. From the analytical expression for the magnetic field produced by a PM, the interacting force between a pair of magnets can be calculated using the Lorentz force law.

In the applications considered here, the PMs are constrained in such a way that their centroids pass through the same line so that only the force along that direction matters. Regarding Fig. 1b, if two PMs are disposed along the $z$-axis, with their magnetization directions along this same axis, the force exerted by $\mathrm{PM}_1$ over $\mathrm{PM}_2$ can be evaluated as:

$$\mathbf{F}_{\mathrm{PM}}(\boldsymbol{\delta}) = \hat{\mathbf{z}}\frac{B_{r_1}B_{r_2}}{4\pi\mu_0}\sum_{i=0}^{1}\sum_{j=0}^{1}\sum_{k=0}^{1}\sum_{l=0}^{1}\sum_{m=0}^{1}\sum_{n=0}^{1}(-1)^{i+j+k+l+m+n}\phi(u,v,w), \tag{1}$$

where $\mu_0$ is the permeability of free space, $B_{r_\mathrm{i}}$ is the residual magnetic flux density (or remanence) of $\mathrm{PM_i}$, and $\boldsymbol{\delta} = \begin{Bmatrix} x & y & z \end{Bmatrix}^{\mathrm{T}}$ is the displacement of $\mathrm{PM}_2$ relative to $\mathrm{PM}_1$. This expression holds when the PMs are attracting each other.

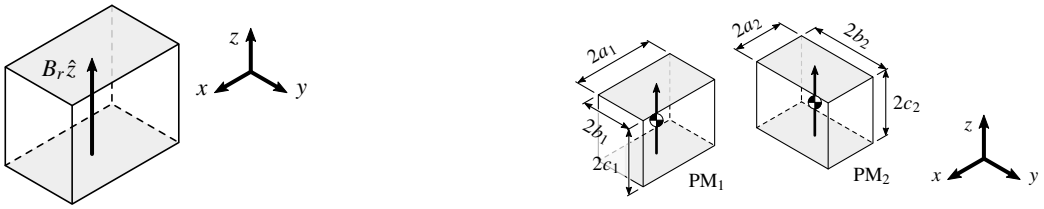


(a) Surface charge model and magnetization of the PM.

(b) Dimensions of the PMs.

Figure 1: Surface charge model and the dimensions of the PMs.

In the event that they are repelling each other, a minus sign must be added to Eq. (1). The function $\phi(u, v, w)$ reads:

$$\phi(u,v,w) = -uw\ln(r-u) - vw\ln(r-v) + uv\tan^{-1}\left(\frac{uv}{rw}\right) - rw, \tag{2}$$

with the intermediate variables $u$, $v$, $w$ and $r$ depending on the dimensions and displacements between the PMs:

$$u = x - (-1)^i a_1 + (-1)^j a_2, \qquad v = y - (-1)^k b_1 + (-1)^l b_2, \qquad w = z - (-1)^m c_1 + (-1)^n c_2,$$
$$r = \sqrt{u^2+v^2+w^2}. \tag{3}$$

As shown in Fig. 1b, $2a_i$, $2b_i$ and $2c_i$ are the dimensions of the $\text{PM}_i$.

### 2.2. Harmonic Balance Method applied to wave propagation in periodic structures

In order to present the HBM for wave propagation in periodic structures, the equations of motion for the unit cell indexed by the integer $n$ are initially stated:

$$\mathbf{M}\frac{\mathrm{d}^2\mathbf{u}^{(n)}}{\mathrm{d}t^2} + \mathbf{f}_{\mathrm{NL}}\left(\mathbf{u}^{(n)}, \mathbf{u}^{(n\pm1)}, \frac{\mathrm{d}\mathbf{u}^{(n)}}{\mathrm{d}t}, \frac{\mathrm{d}\mathbf{u}^{(n\pm1)}}{\mathrm{d}t}\right) = \mathbf{0}, \tag{4}$$

where $\mathbf{M}$ is the mass matrix, and $\mathbf{f}_{\mathrm{NL}}$ is a vector related to both linear and nonlinear interaction forces. The vector $\mathbf{u}^{(n)} = \left\{u_1^{(n)} \quad u_2^{(n)} \quad \cdots \quad u_N^{(n)}\right\}^{\mathrm{T}}$ contains the $N$ generalized coordinates of the $n$-th unit cell. In Eq. (4), it is assumed that interactions only occur between the nearest neighbors.

In accordance with the HBM, the following ansatz is considered (Narisetti *et al.*, 2012):

$$\mathbf{u}^{(n)} = A\sum_{h=1}^{H}\left\{\mathbf{c}_h\cos[h(\mathbf{k}\cdot\mathbf{r}_n + \omega t)] + \mathbf{s}_h\sin[h(\mathbf{k}\cdot\mathbf{r}_n + \omega t)]\right\}, \tag{5}$$

where $A$ is the wave amplitude, $\mathbf{c}_h = \left\{c_{h1} \quad c_{h2} \quad \cdots \quad c_{hN}\right\}^{\mathrm{T}}$ and $\mathbf{s}_h = \left\{s_{h1} \quad s_{h2} \quad \cdots \quad s_{hN}\right\}^{\mathrm{T}}$ are the cosine and sine Fourier coefficients of the approximation, $\mathbf{r}_n$ is the position vector of the $n$-th unit cell with respect to an arbitrary reference point, and $H$ is the number of harmonics considered in the ansatz. The previous equation assumes that the solution of Eq. (4) can be cast in the form of a truncated Fourier series. Physically, it represents a superposition of $H$ plane waves with wave vectors $\mathbf{k},\ 2\mathbf{k},\ \ldots,\ H\mathbf{k}$ and frequencies $\omega,\ 2\omega,\ \ldots,\ H\omega$.

Equation (5) can be written in terms of the propagation vector $\boldsymbol{\mu}$ by realizing that $\mathbf{k}\cdot\mathbf{r}_n = \boldsymbol{\mu}\cdot\mathbf{n}$, where $\boldsymbol{\mu}\cdot\mathbf{n} = \mu l n$ in the considered one dimensional case, with $\mu$ being the component of the wave vector $\mathbf{k}$ in the reciprocal basis, and $l$ being the length of the unit cell (Brillouin, 2003; Hussein *et al.*, 2014). This way, Eq. (5) can be rewritten as:

$$\mathbf{u}^{(n)} = A\sum_{h=1}^{H}\left\{\mathbf{c}_h\cos[h(\boldsymbol{\mu}\cdot\mathbf{n} + \omega t)] + \mathbf{s}_h\sin[h(\boldsymbol{\mu}\cdot\mathbf{n} + \omega t)]\right\}, \tag{6}$$

or in the matrix form:

$$\mathbf{u}^{(n)} = A\mathbf{h}\left(\boldsymbol{\mu}, \mathbf{n}, \omega, t\right)\hat{\mathbf{q}}, \tag{7}$$

where $\hat{\mathbf{q}}$, which collects all Fourier coefficients of the ansatz, can be written as $\hat{\mathbf{q}} = \left\{\hat{\mathbf{q}}_1^{\mathrm{T}} \quad \hat{\mathbf{q}}_2^{\mathrm{T}} \quad \cdots \quad \hat{\mathbf{q}}_H^{\mathrm{T}}\right\}^{\mathrm{T}}$. Each vector $\hat{\mathbf{q}}_j$ collects the $j$-th harmonic Fourier coefficients of all degrees of freedom, and can be written as:

$$\hat{\mathbf{q}}_j = \left\{c_{j1} \quad s_{j1} \quad c_{j2} \quad s_{j2} \quad \cdots \quad c_{jN} \quad s_{jN}\right\}^{\mathrm{T}}, \qquad j = 1, \ldots, H, \tag{8}$$

where $c_{jd}$ and $s_{jd}$ are related to the $j$-th harmonic of the generalized coordinate $u_d^{(n)}$. The matrix $\mathbf{h}\left(\boldsymbol{\mu}, \mathbf{n}, \omega, t\right)$ can be compactly written as:

$$\mathbf{h}\left(\boldsymbol{\mu}, \mathbf{n}, \omega, t\right) = \check{\mathbf{h}}\left(\boldsymbol{\mu}, \mathbf{n}, \omega, t\right) \otimes \mathbf{I}_N, \tag{9}$$

where $\mathbf{I}_N$ is the identity matrix of size $N \times N$, $\otimes$ denotes the Kronecker product between matrices, and $\check{\mathbf{h}}$ is given by:

$$\check{\mathbf{h}}\left(\boldsymbol{\mu}, \mathbf{n}, \omega, t\right) = \big[\cos(\boldsymbol{\mu}\cdot\mathbf{n}+\omega t) \quad \sin(\boldsymbol{\mu}\cdot\mathbf{n}+\omega t) \quad \cos(2(\boldsymbol{\mu}\cdot\mathbf{n}+\omega t)) \quad \sin(2(\boldsymbol{\mu}\cdot\mathbf{n}+\omega t)) \quad \cdots \\ \cdots \quad \cos(H(\boldsymbol{\mu}\cdot\mathbf{n}+\omega t)) \quad \sin(H(\boldsymbol{\mu}\cdot\mathbf{n}+\omega t))\big]. \tag{10}$$

Substituting Eq. (7) into Eq. (4) yields the following residual:

$$\mathbf{r}_H = A\mathbf{M}\frac{\mathrm{d}^2\mathbf{h}}{\mathrm{d}t^2}\hat{\mathbf{q}} + \mathbf{f}_{\mathrm{NL}}\left(A, \boldsymbol{\mu}, \mathbf{n}, \omega, t\right) = \mathbf{0}, \tag{11}$$

where dependencies of $\mathbf{h}(\,\cdot\,)$ have been omitted. With no loss of generality, the index of the reference unit cell is chosen as $n = 0$, such that all dependencies on $\mathbf{n}$ can now be suppressed.

The first time derivative of $\mathbf{h}\left(\boldsymbol{\mu}, \omega, t\right)$ can be computed as:

$$\frac{\mathrm{d}\mathbf{h}}{\mathrm{d}t} = \frac{\mathrm{d}\check{\mathbf{h}}}{\mathrm{d}t}\otimes\mathbf{I}_N = \check{\mathbf{h}}\check{\boldsymbol{\nabla}}\otimes\mathbf{I}_N, \quad \text{with} \quad \check{\boldsymbol{\nabla}} = \omega\,\mathrm{diag}\left(\boldsymbol{\nabla}_1,\ \boldsymbol{\nabla}_2,\ \ldots,\ \boldsymbol{\nabla}_H\right) \quad \text{and} \quad \boldsymbol{\nabla}_k = \begin{bmatrix} 0 & k \\ -k & 0 \end{bmatrix}. \tag{12}$$

Accordingly, the second time derivative of $\mathbf{h}\left(\boldsymbol{\mu}, \mathbf{n}, \omega, t\right)$ can be written as:

$$\frac{\mathrm{d}^2\mathbf{h}}{\mathrm{d}t^2} = \frac{\mathrm{d}^2\check{\mathbf{h}}}{\mathrm{d}t^2}\otimes\mathbf{I}_N = \check{\mathbf{h}}\check{\boldsymbol{\nabla}}^2\otimes\mathbf{I}_N, \tag{13}$$

so that the residual given in Eq. (11) can be compactly rewritten as:

$$\mathbf{r}_H = A\mathbf{M}\left(\check{\mathbf{h}}\check{\boldsymbol{\nabla}}^2\otimes\mathbf{I}_N\right)\hat{\mathbf{q}} + \mathbf{f}_{\mathrm{NL}}\left(A, \boldsymbol{\mu}, \omega, t\right) = \mathbf{0}. \tag{14}$$

Since the proposed ansatz is periodic (cf. Eq. (6), with unknown period $T$, in this autonomous case), so is the established residual $\mathbf{r}_H$. Hence, it can also be represented by a Fourier series. Due to the nonlinearities present in the equations of motion, harmonics of order higher than $H$ may exist in $\mathbf{r}_H$. Loosely speaking, the less smooth the nonlinearities, the more harmonics will be present in $\mathbf{f}_{\mathrm{NL}}$ and, consequently, in $\mathbf{r}_H$. The HBM requires that the Fourier coefficients of this residual are zero until the order of truncation of the ansatz, $H$. This can be mathematically stated as:

$$\hat{\mathbf{r}}_H = \frac{1}{T}\int_0^T \mathbf{h}^{\mathrm{T}}\mathbf{r}_H\,\mathrm{d}t = A\left[\frac{1}{T}\int_0^T \mathbf{h}^{\mathrm{T}}\mathbf{M}\left(\check{\mathbf{h}}\check{\boldsymbol{\nabla}}^2\otimes\mathbf{I}_N\right)\mathrm{d}t\right]\hat{\mathbf{q}} + \frac{1}{T}\int_0^T \mathbf{h}^{\mathrm{T}}\mathbf{f}_{\mathrm{NL}}\left(A, \boldsymbol{\mu}, \mathbf{n}, \omega, t\right)\mathrm{d}t = \mathbf{0}. \tag{15}$$

The time integration removes the temporal dependence of $\mathbf{r}_H$, so that Eq. (15) is purely algebraic. Due to the orthogonality properties of the Fourier basis functions, it can be shown that the Fourier coefficients of the linear term can be simplified to (Krack and Gross, 2019):

$$\frac{1}{T}\int_0^T \mathbf{h}^{\mathrm{T}}\mathbf{M}\left(\check{\mathbf{h}}\check{\boldsymbol{\nabla}}^2\otimes\mathbf{I}_N\right)\mathrm{d}t = \check{\boldsymbol{\nabla}}^2\otimes\mathbf{M}, \tag{16}$$

so that Eq. (15) can be written as:

$$\hat{\mathbf{r}}_H = A\left(\check{\boldsymbol{\nabla}}^2\otimes\mathbf{M}\right)\hat{\mathbf{q}} + \hat{\mathbf{f}}_{\mathrm{NL}} = \mathbf{0}, \qquad \text{with} \qquad \hat{\mathbf{f}}_{\mathrm{NL}} = \frac{1}{T}\int_0^T \mathbf{h}^{\mathrm{T}}\mathbf{f}_{\mathrm{NL}}\left(A, \boldsymbol{\mu}, \omega, t\right)\mathrm{d}t. \tag{17}$$

The vector $\hat{\mathbf{f}}_{\mathrm{NL}}$ can be recognized as the Fourier coefficients of the nonlinear forces vector, and its computation is addressed in the following.

### 2.3. The Alternating Frequency-Time method

Although the Fourier coefficients of the linear portion of the residue can be treated analytically with relative ease through Eq. (16), those associated with nonlinear forces are difficult (or even impossible) to determine in a closed form. This is especially true for intricate nonlinearities and/or large values of $H$. In these cases, one must resort to approximate numerical solutions.

A scheme widely used in conjunction with the standard HBM is the AFT scheme (Cameron and Griffin, 1989), which makes use of the computationally efficient Fast Fourier Transform (FFT) algorithm (in its direct and inverse forms) to approximate the Fourier coefficients of the nonlinear term. The AFT scheme is illustrated in Fig. 2. When solving the nonlinear algebraic equations given in Eq. (17), an iterative solution procedure (e.g., the Newton-Raphson method) is usually adopted. So, at the beginning of the solution algorithm, an initial guess for the unknown vector $\hat{\mathbf{q}}$ needs to be

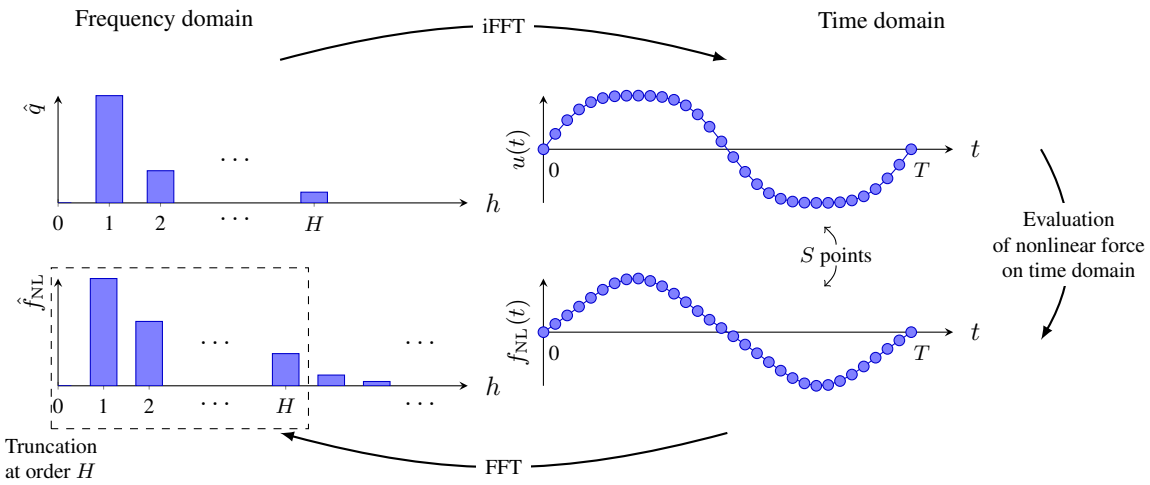


Figure 2: Alternating frequency-time scheme.

provided. Under the AFT framework, this guess is first converted to the time domain using the inverse FFT algorithm, producing $\mathbf{u}^{(n)}(t_k)$ for $t_k \in [0, T)$. If the vector of nonlinear forces also depends on the generalized velocities, the time derivative of $\mathbf{u}^{(n)}$ can first be computed in the frequency domain, and then transformed to the time domain in order to produce $\dot{\mathbf{u}}^{(n)}$. In addition, if nonlinear forces are present in the coupling between unit cells, the generalized displacements of neighboring cells $\mathbf{u}^{(n\pm1)}$ and, possibly, their generalized velocities $\dot{\mathbf{u}}^{(n\pm1)}$, must also be calculated. Again, this can be accomplished by first evaluating Fourier coefficients in the frequency domain and, then, transforming the results to the time domain. Once $\mathbf{u}^{(n)}$, $\dot{\mathbf{u}}^{(n)}$, $\mathbf{u}^{(n\pm1)}$ and $\dot{\mathbf{u}}^{(n\pm1)}$ are available, $\mathbf{f}_{\mathrm{NL}}$ can be computed directly in the time domain. Afterwards, it can be readily be converted to the frequency domain using the direct FFT, generating an approximation for $\hat{\mathbf{f}}_{\mathrm{NL}}$. With this vector available, the iterative process can continue by calculating the residue cf. Eq. (17).

An important aspect of the AFT scheme is the number $S$ of sampling points taken into consideration for computing the displacements and velocities $\mathbf{u}^{(n+j)}$ and $\dot{\mathbf{u}}^{(n+j)}$, $j = 0, \pm1$. Even if, say, $x(t)$ can be represented exactly by a truncated Fourier series with truncation order $H$, a nonlinear function $f_{\mathrm{NL}}(x(t))$ generates, in general, an infinite set of harmonics, so that its sampling inevitably leads to aliasing. However, in the particular case of polynomial nonlinearity (which is by far the most studied type of nonlinearity in the dispersion analysis of periodic structures), $f_{\mathrm{NL}}(x(t))$ can exactly be represented by a truncated Fourier series. Due to the convolution theorem, when two truncated Fourier series are multiplied, their truncation orders add. So, if $x(t)$ can be represented exactly by a truncated Fourier series with truncation order $H$, a polynomial nonlinear function $f_{\mathrm{NL}}(x(t)) = x^{\kappa}(t)$ has an exact Fourier series representation with truncation order $\kappa H$. This way, the AFT scheme gives the exact Fourier coefficients for this particular $f_{\mathrm{NL}}$ provided that at least $2\kappa H + 1$ samples are used to sample $x(t)$.

For forces described by non-polynomial functions, however, a large $S$ may be required to minimize the aliasing effect. Although the number of time samples does not affect the size of the HBM residue equation, it affects the computation time of the direct and inverse DFTs in the AFT scheme. Commonly, $S$ is taken to be an integer power of 2, since in this case the FFT algorithm reaches its maximum computational efficiency. In practice, a convergence study can be carried out to determine a reasonable $S$ value that balances accuracy and computational efficiency.

### 2.4. Phase condition and amplitude normalization

Since the model assumed for investigating free wave propagation on periodic structures does not depend explicitly on time, if $\mathbf{u}^{(n)}(t)$ is a periodic solution of the autonomous system given in Eq. (4), so is $\mathbf{u}^{(n)}(t + \Delta t)$, for any $\Delta t$. Accordingly, to remove the arbitrariness of the initial condition, a phase condition has to be taken into account. Different constraints for the phase have been proposed in the literature (Seydel, 2010). Here, one adopts:

$$r_{\text{phase}} = \dot{u}^{(n)}_{i_{\text{phase}}}\Big|_{t=0} = 0, \tag{18}$$

where the index $i_{\text{phase}}$ must be selected in such a way that $\dot{u}^{(n)}_{i_{\text{phase}}}(t)$ is not identically zero throughout the period $T$.

While specification of the initial phase of the solution is required to address arbitrariness, as just discussed, another point also needs attention: one must constraint the amplitude of the vector $\hat{\mathbf{q}}$. The choice of an amplitude normalization strategy directly impacts the actual amplitude of $\mathbf{u}^{(n)}$, cf. Eq. (7). Different normalizations have been proposed in the literature. Narisetti *et al.* (2012) normalized $\hat{\mathbf{q}}$ such that its first coefficient is equal to 1, i.e. $c_{11} = 1$ (cf. Eq. (8)). A similar approach was considered by Song and Zhu (2021) and Wei *et al.* (2020), who have adopted $c_{11} = A$.

Undoubtedly, these normalization procedures are quite simple and easy to implement. Nevertheless, besides removing an unknown of the problem, they can lead to inconsistencies. For example, for certain wavenumber values, the corresponding component of an eigenvector of the linearized system can be equal to 0. If this is the case, it is not possible to normalize such an eigenvector so that it has $c_{11} = 1$ or $c_{11} = A$. Since the eigenvectors of the linearized system are used as initial guesses for $\hat{\mathbf{q}}$, convergence issues can be encountered for particular values of wavenumber.

Furthermore, with the preceding amplitude normalization strategies, one might not be able to recover the eigensolutions related to the linearized system through the resolution of Eq. (17), which is what should be expected for small wave amplitudes. One therefore considers the following normalization condition for $\hat{\mathbf{q}}$:

$$r_{\text{norm}} = \hat{\mathbf{q}}^{\mathrm{T}}\hat{\mathbf{q}} - 1 = 0. \tag{19}$$

### 2.5. Numerical computation of the amplitude-dependent dispersion diagram

Previously, the autonomous differential equations given in Eq. (4) were converted to a system of nonlinear algebraic equations, cf. Eq. (17), by employing the HBM. Equation (17) consists of a set of $2HN$ nonlinear algebraic equations. Accordingly, the vector of Fourier coefficients $\hat{\mathbf{q}}$ possesses $2HN$ unknowns. Additional equations are the phase condition, given by Eq. (18), and the amplitude normalization constraint, seen in Eq. (19). In the autonomous case, which is the one considered here, the frequency $\omega$ is also an unknown.

The numerical procedure proposed to compute the dispersion diagram relating the propagation vector $\boldsymbol{\mu}$ to the frequency $\omega$ calls for specifying a wave amplitude $A$ and varying the components of $\boldsymbol{\mu}$ within the first irreducible Brillouin zone. Mathematically, this can be accomplished by solving the set of $2HN + 2$ nonlinear algebraic equations $\mathbf{R}(\mathbf{x}) = \left\{\hat{\mathbf{r}}_H^{\mathrm{T}} \quad r_{\text{norm}} \quad r_{\text{phase}}\right\}^{\mathrm{T}} = \mathbf{0}$ with respect to the $2HN + 1$ unknowns collected in $\mathbf{x} = \left\{\hat{\mathbf{q}}^{\mathrm{T}} \quad \omega\right\}^{\mathrm{T}}$. The numerical procedure adopted is outlined below:

1. Choose a value for the wave amplitude $A$.
2. Select the number $H$ of harmonics to be considered in the ansatz given by Eq. (6).
3. Choose the number $S$ of sampling points to be considered in the AFT scheme. This may require a convergence study to avoid the selection of an unnecessarily large value.
4. Select a branch of the dispersion diagram to study and choose the index $i_{\text{phase}}$ to perform phase normalization (cf. Eq. (18)).
5. Select the components of the propagation vector $\boldsymbol{\mu}$ within the first irreducible Brillouin zone.
6. For the propagation vector of step 5, solve the eigenproblem associated to the linearized system to determine the eigenvalue $\omega_{\text{lin}}$ and the eigenvector $\mathbf{u}_{\text{lin}}$ related to the branch under consideration. This eigenvector must be normalized using Eqs. (18) and (19). The eigenvalue $\omega_{\text{lin}}$ is used as an initial guess for the wave frequency $\omega$. The normalized eigenvector $\mathbf{u}_{\text{lin}}$ serves as an initial guess for the coefficients related to the fundamental harmonic of the vector $\hat{\mathbf{q}}$. To make the representations of $\mathbf{u}_{\text{lin}}$ (which is complex, in general) and $\hat{\mathbf{q}}$ (which is real) compatible, one must set $\left\{c_{11} \quad c_{12} \quad \cdots \quad c_{1N}\right\}^{\mathrm{T}} = \Re(\mathbf{u}_{\text{lin}})$ and $\left\{s_{11} \quad s_{12} \quad \cdots \quad s_{1N}\right\}^{\mathrm{T}} = -\Im(\mathbf{u}_{\text{lin}})$. The initial guesses for the coefficients of $\hat{\mathbf{q}}$ related to higher harmonics can be set equal to 0.
7. Provide the initial guess to a solver of nonlinear algebraic equations, along with a script that evaluates $\mathbf{R}(\mathbf{x})$ for a given $\mathbf{x}$. The solver is expected to evaluate $\mathbf{x}_{\text{sol}} = \left\{\hat{\mathbf{q}}_{\text{sol}}^{\mathrm{T}} \quad \omega_{\text{sol}}\right\}^{\mathrm{T}}$ such that $\mathbf{R}(\mathbf{x}_{\text{sol}}) \approx \mathbf{0}$, according to the adopted stopping criteria. The plot of $\boldsymbol{\mu}$ against $\omega_{\text{sol}}$ provides a point of the desired amplitude-dependent dispersion diagram.
8. Return to step 5 and repeat the analysis for a new value of $\boldsymbol{\mu}$.

For large values of amplitude $A$, it may be necessary to first analyze conditions with smaller values of $A$, for which the linear eigensolutions are closer to the solutions of the corresponding nonlinear problems. The solutions for smaller values of $A$, in which the nonlinear effects are less pronounced, can then be used as initial guesses for the solutions sought for larger values of wave amplitude. Analogously, solutions considering higher order harmonics can be sought using as initial guesses the solutions for the nonlinear problems considering harmonics of lower order.

## 3. NUMERICAL EXPERIMENTS AND DISCUSSION

In this section, the above-discussed methodology is applied to the study of free wave propagation of monoatomic lattice structures comprised of PMs on an elastic foundation. The PMs are arranged in two different ways, such that configurations with both repelling and attracting interaction forces are achieved. The material, elastic and geometric parameters adopted for the lattice in both cases are the same, and are reported in Tab. 1.

Regarding the AFT scheme, the parameter $S$ was chosen equal to $2^8$ points. Since the lattices under analysis are monoatomic, the only possible choice for $i_{\text{phase}}$ is $i_{\text{phase}} = 1$.

In all analysis, the amplitude-dependent dispersion relation is evaluated for 100 values of the propagation constant $\mu$, equally spaced within the first irreducible Brillouin zone.

Table 1: Lattice features adopted for simulations.

| Parameter | Description | Value |
|---|---|---|
| $a$, $b$, $c$ | Dimensions of the PMs | 3.175 mm |
| $k_f$ | Elastic foundation stiffness | 230 N/m |
| $m$ | Mass of the PMs | 5 g |
| $\mu_0$ | Permeability of free space | $4\pi \cdot 10^{-7}$ H/m |
| $B_r$ | residual magnetic flux density | 1.3098 T |
| $l$ | length of the unit cell | 20 mm |

### 3.1. Monoatomic repelling magnetoelastic chain

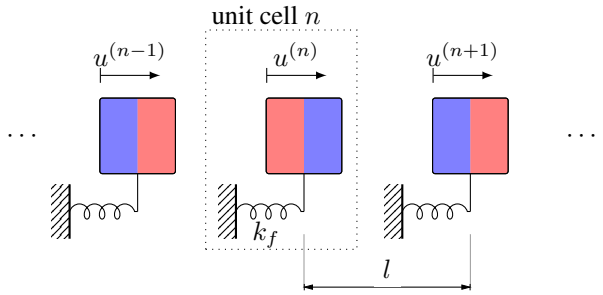


Figure 3: Monoatomic magnetoelastic chain of repelling PMs on an elastic foundation.

The first numerical experiment considers the monoatomic chain shown in Fig. 3, whose unit cell is made up of cubic PMs attached to the ground through a linear spring. The PMs are spatially oriented such that their magnetization direction (cf. Fig. 1) is aligned with the axis of the chain. Moreover, PMs which are neighbors repel each other.

The equation of motion for the $n$-th unit cell can be written as:

$$m\frac{\mathrm{d}^2u^{(n)}}{\mathrm{d}t^2} + k_f u^{(n)} + f_{\mathrm{NL}}\left(u^{(n)}, u^{(n-1)}, u^{(n+1)}\right) = 0, \tag{20}$$

where $m$ is the mass of the PM, $k_f$ is the elastic foundation stiffness and $f_{\mathrm{NL}}\left(u^{(n)}, u^{(n-1)}, u^{(n+1)}\right)$ represents the forces of interaction between the PM of the $n$-th unit cell and those of the adjacent cells, which can be assessed through Eq. (1).

Equation (20) can be linearized using a Taylor series expansion around the point at which the system is at rest, which is an equilibrium point. By doing this, a linear dispersion analysis can be easily performed. For the nonlinear case, in which the free wave propagation is amplitude-dependent, the dispersion relation is evaluated for wave amplitudes $A =$ 1%, 5%, 10%, 15% and 20% of $\delta_0$, where $\delta_0 = l - 2c$ is the distance between the faces of consecutive PMs when they are at rest.

The dispersion diagram of the linearized system, as well as the amplitude-dependent dispersion relations of the nonlinear chain are shown in Fig. 4. These results were obtained by considering $H = 1$. For small values of the wave amplitude $A$, the dispersion relation of the nonlinear configuration is close to the one obtained for the linearized system, as expected. An increase in wave amplitude leads to an increase in the nonlinear character of the forces between the PMs, so that the dispersion diagram of the nonlinear chain moves farther and farther away from the one computed for the linearized version of the lattice as the wave amplitude increases. The shift of the upper cutoff frequency to higher values shows that the repelling magnetoelastic chain presents a hardening behavior (Narisetti *et al.*, 2010).

A convergence study for the number $H$ of harmonics considered in the HBM ansatz is shown in Fig. 5. The figure shows the dispersion diagram for $A = 20\%$ of $\delta_0$ considering $H = 1, 2, 10$. From this figure, it can be seen that a single harmonic is enough to accurately capture the shift in the dispersion diagram related to the nonlinear lattice structure. Furthermore, it is noticed that the discrepancies are smaller for the values of $\mu$ near the boundaries of the first irreducible Brillouin zone, which are the ones that dictate the cutoff frequencies in this case. Thus, the difference between the results for $H = 1$ and $H = 10$ are considered negligible here, and this justifies the choice of $H = 1$ for the results shown in Fig. 4. Also because of this, the results shown in the remainder of this paper have been obtained considering $H = 1$.

### 3.2. Monoatomic attracting magnetoelastic chain

The next example deals with a monoatomic magnetoelastic chain on an elastic foundation, just as before. In this case, however, the spatial arrangement of the PMs is changed so that they are attracting each other, as shown in Fig. 6. The

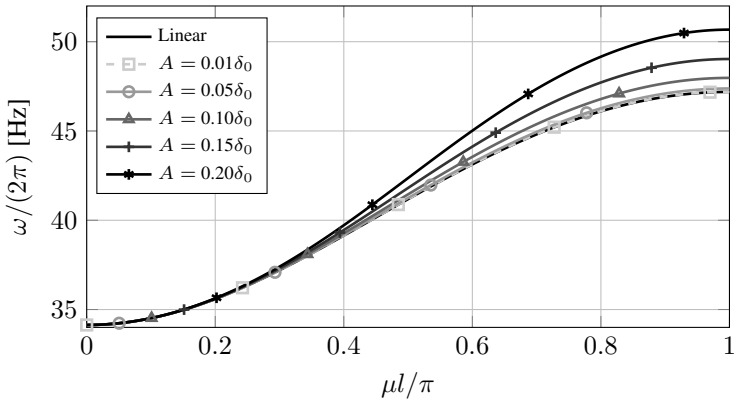


Figure 4: Amplitude-dependent dispersion diagram of a monoatomic repelling magnetoelastic chain. Results obtained using the proposed AFT-HBM methodology, considering $H = 1$.

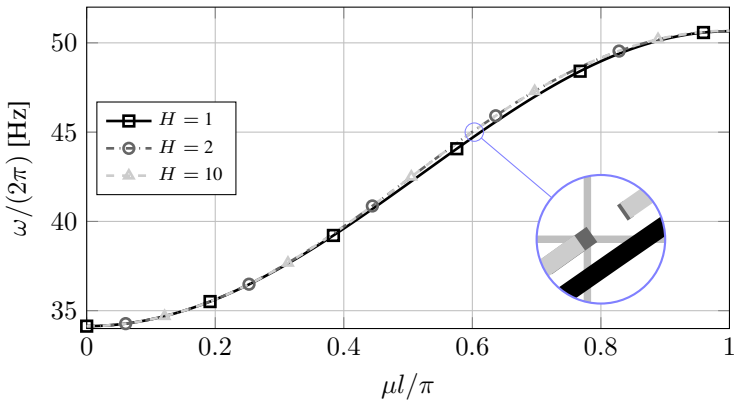


Figure 5: Dispersion diagram of a monoatomic repelling magnetoelastic chain obtained using the AFT-HBM methodology, considering $A = 0.20\,\delta_0$ and $H = 1$, 2 and 10.

equation of motion for the $n$-th unit cell is similar to Eq. (20), but with the sign of the function related to the magnetic interactions' forces changed:

$$m\frac{\mathrm{d}^2u^{(n)}}{\mathrm{d}t^2} + k_f u^{(n)} - f_{\mathrm{NL}}\left(u^{(n)}, u^{(n-1)}, u^{(n+1)}\right) = 0, \tag{21}$$

where the parameters are the same as before.

Again, the dispersion relation of the underlying linearized system can be found by performing a Taylor series expansion of Eq. (21) around the initial equilibrium state, followed by the solution of the eigenproblem which ensues. For the nonlinear case, in which the free wave propagation is amplitude-dependent, the dispersion relation is evaluated for the wave amplitudes $A = 1\%$, $5\%$, $10\%$, $15\%$ and $20\%$ of $\delta_0$, just as before.

The dispersion diagram of the linearized system, as well as the amplitude-dependent dispersion relations of the nonlinear chain are shown in Fig. 7. These results were obtained by considering $H = 1$. For small values of the wave amplitude $A$, the dispersion relations associated to the nonlinear chain are close to the one obtained for its linearized counterpart, as

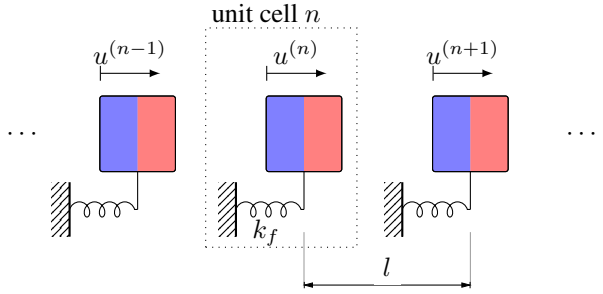


Figure 6: Monoatomic magnetoelastic chain of attracting PMs on an elastic foundation.

expected. An increase in wave amplitude leads to an increase in the nonlinear character of the forces between the PMs, so that the dispersion diagrams of the nonlinear chain move farther and farther away from the one obtained for the linearized system as $A$ increases. In this case, however, the lower cutoff frequency shifts to smaller values, which shows that the attracting magnetoelastic chain possesses a softening nonlinear behavior (Narisetti *et al.*, 2010).

Figure 7 also shows that for larger wave amplitudes and certain values of the propagation constant, the dispersion diagram reaches zero frequency, so that there is no free wave propagation. This behavior can be explained by analyzing the equivalent stiffness of the system. It is widely known that softening-type springs are characterized by negative stiffness. Therefore, as the wave amplitude increases, the softening stiffness of the attracting magnetic force increases in importance.This causes the equivalent stiffness of the system, which includes the elastic foundation stiffness, to be negative for certain propagation constant values. Then, no wave is allowed to propagate freely. A similar behavior has already been reported for a weakly nonlinear periodic system with active control performed by a piezoelectric spring (Wang and Wang, 2018).

To highlight the relevance of this behavior, the analysis has been repeated by changing the unit cell length from $l = 20$ mm to $l = 19$ mm. As shown in Fig. 7, even the linearized case has a negative equivalent stiffness for certain values of the propagation constant. By increasing the wave amplitude, the dispersion diagram shifts to lower frequency values, so that free wave propagation is only allowed for increasingly smaller values of $\mu$.

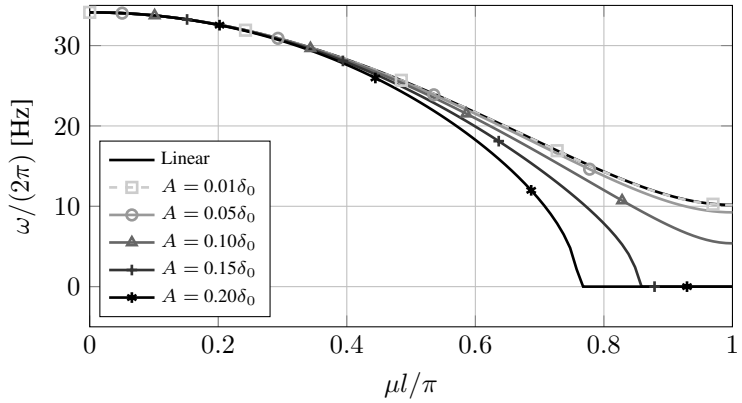


Figure 7: Amplitude-dependent dispersion diagram for a monoatomic attracting magnetoelastic chain. Results obtained through AFT-HBM considering $H = 1$.

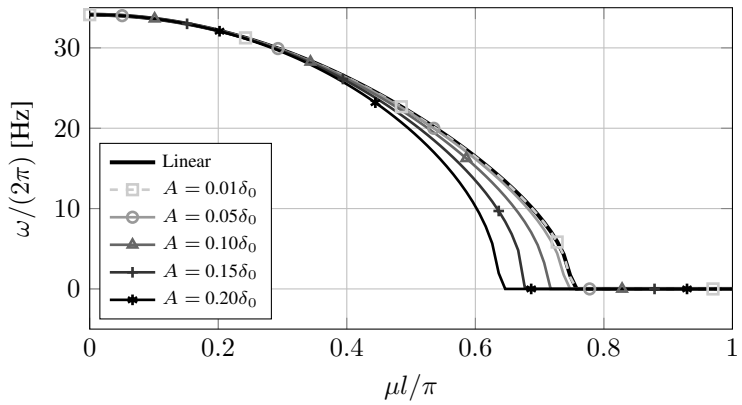


Figure 8: Amplitude-dependent dispersion diagram for a monoatomic attracting magnetoelastic chain. In this case, the length $l$ of the unit cell is made 1 mm smaller. Results obtained through AFT-HBM considering $H = 1$.

## 4. CONCLUDING REMARKS

This paper presented a new methodology for computing the dispersion diagram of strongly nonlinear periodic structures, which are shown to exhibit amplitude-dependence. The method is based on the Harmonic Balance Method adapted to free wave propagation problems. To assess the influence of the nonlinear forces, the use of the Alternating Frequency-Time was proposed. The importance of the phase condition and amplitude normalization for autonomous equations was discussed and a suitable choice for these quantities was proposed. Finally, the methodology was illustrated through the study of monoatomic lattice structures composed of permanents magnets on an elastic foundation. Configurations with both repelling and attracting forces between the PMs were studied, which showed hardening and softening behavior, re-

spectively. The proposed HBM-AFT strategy proved to be able to predict the dispersion relation of strongly nonlinear periodic structures.

**Acknowledgements**

M.B.R.Fernandes is grateful to the São Paulo State Research Foundation (FAPESP) for his doctorate scholarship (grant #19/19921-5). All authors also acknowledge FAPESP for supporting their work through a thematic grant (Periodic structure design and optimization for enhanced vibroacoustic performance: ENVIBRO, #18/15894-0). D.A.Rade acknowledges the Brazilian Research Council (CNPq) for grants #310633/2013-3 and #312068/2020-4.

## 5. REFERENCES

Brillouin, L., 2003. *Wave Propagation in Periodic Structures: Electric Filters and Crystal Lattices*. Dover phoenix editions. Dover Publications. ISBN 9780486495569.

Cabaret, J., Tournat, V. and Béquin, P., 2012. "Amplitude-dependent phononic processes in a diatomic granular chain in the weakly nonlinear regime". *Physical Review E*, Vol. 86, No. 4.

Cameron, T.M. and Griffin, J.H., 1989. "An alternating frequency/time domain method for calculating the steady-state response of nonlinear dynamic systems". *Journal of Applied Mechanics*, Vol. 56, No. 1, pp. 149–154.

Huang, H., Sun, C. and Huang, G., 2009. "On the negative effective mass density in acoustic metamaterials". *International Journal of Engineering Science*, Vol. 47, No. 4, pp. 610–617. ISSN 0020-7225.

Hussein, M.I., Leamy, M.J. and Ruzzene, M., 2014. "Dynamics of phononic materials and structures: Historical origins, recent progress, and future outlook". *Applied Mechanics Reviews*, Vol. 66, No. 4.

Janssen, J., 2011. *Extended analytical charge modeling for permanent-magnet based devices : practical application to the interactions in a vibration isolation system*. Ph.D. thesis, Electrical Engineering.

Krack, M. and Gross, J., 2019. *Harmonic Balance for Nonlinear Vibration Problems*. Springer International Publishing.

Laude, V., 2020. *Phononic Crystals*. De Gruyter.

Liu, Z., 2000. "Locally resonant sonic materials". *Science*, Vol. 289, No. 5485, pp. 1734–1736.

Manktelow, K., Narisetti, R.K., Leamy, M.J. and Ruzzene, M., 2013. "Finite-element based perturbation analysis of wave propagation in nonlinear periodic structures". *Mechanical Systems and Signal Processing*, Vol. 39, No. 1-2, pp. 32–46.

Manktelow, K.L., Leamy, M.J. and Ruzzene, M., 2014. "Analysis and experimental estimation of nonlinear dispersion in a periodic string". *Journal of Vibration and Acoustics*, Vol. 136, No. 3.

Manktelow, K.L., Ruzzene, M. and Leamy, M.J., 2017. *Wave Propagation in Nonlinear Lattice Materials*, John Wiley & Sons, Ltd, pp. 107–137.

Narisetti, R.K., Ruzzene, M. and Leamy, M.J., 2011. "A perturbation approach for analyzing dispersion and group velocities in two-dimensional nonlinear periodic lattices". *Journal of Vibration and Acoustics*, Vol. 133, No. 6.

Narisetti, R.K., Leamy, M.J. and Ruzzene, M., 2010. "A perturbation approach for predicting wave propagation in one-dimensional nonlinear periodic structures". *Journal of Vibration and Acoustics*, Vol. 132, No. 3.

Narisetti, R.K., Ruzzene, M. and Leamy, M.J., 2012. "Study of wave propagation in strongly nonlinear periodic lattices using a harmonic balance approach". *Wave Motion*, Vol. 49, No. 2, pp. 394–410.

Seydel, R., 2010. *Practical Bifurcation and Stability Analysis*. Springer New York.

Song, M. and Zhu, W., 2021. "Elastic wave propagation in strongly nonlinear lattices and its active control". *Journal of Applied Mechanics*, Vol. 88, No. 7.

Theocharis, G., Boechler, N. and Daraio, C., 2013. *Nonlinear Periodic Phononic Structures and Granular Crystals*, Springer Berlin Heidelberg, pp. 217–251.

Wang, X., 2014. "Dynamic behaviour of a metamaterial system with negative mass and modulus". *International Journal of Solids and Structures*, Vol. 51, No. 7-8, pp. 1534–1541.

Wang, X., Zhu, W. and Liu, M., 2020. "Steady-state periodic solutions of the nonlinear wave propagation problem of a one-dimensional lattice using a new methodology with an incremental harmonic balance method that handles time delays". *Nonlinear Dynamics*, Vol. 100, No. 2, pp. 1457–1467.

Wang, Y.Z. and Wang, Y.S., 2018. "Active control of elastic wave propagation in nonlinear phononic crystals consisting of diatomic lattice chain". *Wave Motion*, Vol. 78, pp. 1–8.

Wei, L.S., Wang, Y.Z. and Wang, Y.S., 2020. "Nonreciprocal transmission of nonlinear elastic wave metamaterials by incremental harmonic balance method". *International Journal of Mechanical Sciences*, Vol. 173, p. 105433.

## 6. RESPONSIBILITY NOTICE

The authors are solely responsible for the printed material included in this paper.